Demosaicing Algorithm using High-order Interpolation with Sobel Operators

Mingyu Baek and Jechang Jeong

***Abstract*— To decrease price and size, most digital cameras use single sensor array. Single sensor array acquires only one of three colors at each pixel. Therefore, the missing two color values should be estimated to acquire full color image. To interpolate missing pixels, many demosaicing algorithms have been proposed. In this paper, we proposed improved method based on high-order interpolation. The calculation of gradients is achieved by Sobel operator. As compared with the latest demosaicing algorithms, the proposed algorithm produces the best average CPSNR and subjective quality.**

***Index Terms*—Bayer color filter array, demosaicing, high-order interpolation, Sobel operator.**

I. Introduction

DIGITAL color images consist of three color values at each pixel. Originally, three distinct sensors for each color are needed to represent full color image. However, having three sensor causes price and size of digital camera to increase. Therefore, most digital cameras use single sensor array to be effective. Single sensor array acquires only one of three color at each pixel.

The commonly used color filter array (CFA) is Bayer pattern as shown in Fig. 1 In Bayer pattern, green channel components are twice as much as red or blue, because human sight is more sensitive to green than red or blue [1]. As mentioned before, only one color is measured at each pixel in CFA. Therefore, the missing two color values should be estimated to acquire full color image. The estimation process is called demosaicing.

The simplest demosaicing algorithm is bi-linear interpolation (BI), in which each color channel is interpolated independently. However, such a method cannot consider image properties and produces some color artifacts. Human sights are sensitive to edges in an image, but BI interpolates pixels across edges and blur fine image details.

To restore more accurate and high quality results, many demosaicing algorithms have been proposed. Most existing demosaicing algorithms are edge-directed interpolation,

Manuscript received July 12, 2014; revised July 28, 2014. This research was supported by the MSIP(Ministry of Science, ICT & Future Planning), Korea, under the ITRC(Information Technology Research Center) support program supervised by the NIPA(National IT Industry Promotion Agency) (NIPA-2014-H0301-14-1018).

M. Baek is with the Department of Electronics and Computer Engineering, Hanyang University, 222, Wangsimni-ro, Seongdong-gu, Seoul, Korea (e-mail: hundredmingyu@gmail.com)

J. Jeong is with the Department of Electronics and Computer Engineering, Hanyang University, 222, Wangsimni-ro, Seongdong-gu, Seoul, Korea (corresponding author to provide phone: +82-2-2220-4369; e-mail: jjeong@hanyang.ac.kr)

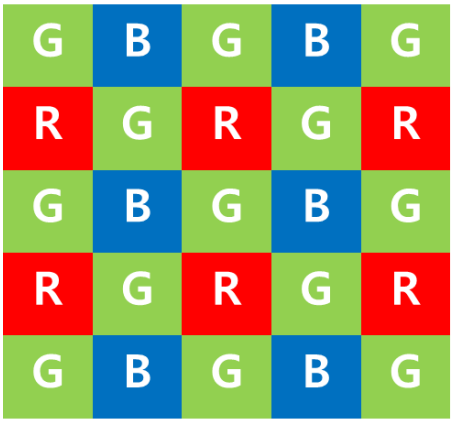

Fig 1. Bayer Pattern

where the gradient is estimated by neighboring pixels to decide the direction. These algorithms can avoid color artifacts that are caused by interpolation across edges. There's common assumption in demosaicing that color ratios or color differences are locally constant within an object of image [2], [3]. This is based on the high correlation between color channels.

Hamilton-Adams [4] adapted the directional Laplacian filter by taking advantage of the interchannel correlation. In recent algorithms, the directional Laplacian filter has been proven to be a good estimator for Bayer CFA. [5] and [7] use this to interpolate the missing channels horizontally or vertically. [5] decide the interpolation direction using the variance of color differences as supplementary information, while [7] proposed integrated gradients which are from color intensity and color difference domains. In [6], they proposed high-order interpolation derived by Taylor series to preserve edges. By including the second-order terms, higher accuracy for the estimates can be achieved.

Although many demosaicing algorithms are proposed, color artifacts in high frequency areas are commonly found in the results of images. To eliminate these artifacts, recent algorithms proposed the additional stage. In this stage, the green channel is enhanced following to the tendency of the color difference domain which is relatively low frequency. Through this stage, it can provide a better reference to interpolate the red and blue channels.

In this paper, we proposed improved method based on high-order interpolation. The remainder of this paper is organized as follows. In section II and III, we explain high-order interpolation and the details of proposed algorithm including each color channel interpolation. Experimental results are presented in section IV. Finally, we conclude the paper in section V.

ISBN: 978-988-19252-0-6
ISSN: 2078-0958 (Print); ISSN: 2078-0966 (Online)

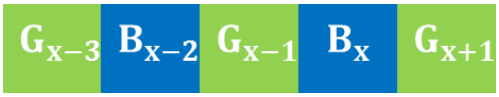

Fig 2. The left-side of Bayer pattern at B_x.

II. HIGH-ORDER INTERPOLATION

In this section, we explain about high-order interpolation. The high-order interpolation is used to get four estimates of missing pixel for four directions. Green channel should be interpolated first, because green channel components are twice as much as red or blue. The left-side estimate is derived by Taylor series [8]

$$g(x) = g(x-1) + g'(x-1) + \frac{1}{2!}g''(x-1) + \cdots + \frac{1}{n!}g^{(n)}(x-1) + \cdots \quad (1)$$

where $g(x)$ means a missing green pixel located at x. To calculate first-order differentiation, we use the central difference approximation

$$g'(x-1) = \frac{g(x) - g(x-2)}{2} = \frac{\bar{G}_x - \bar{G}_{x-2}}{2} \quad (2)$$

where $\bar{G}_x$ and $\bar{G}_{x-2}$ are the values of green pixel located at x and $x-2$, respectively. Based on assumption that color channels are highly correlated within an object of an image, we can approximately replace (2) as follows:

$$g'(x-1) = \frac{\bar{G}_x - \bar{G}_{x-2}}{2} \cong \frac{B_x - B_{x-2}}{2}. \quad (3)$$

For second-order differentiation, we also use the central difference approximation

$$g'(x) = \frac{g(x+1) - g(x-1)}{2} \quad (4)$$

$$g'(x-2) = \frac{g(x-1) - g(x-3)}{2} \quad (5)$$

$$g''(x-1) = \frac{g'(x) - g'(x-2)}{2}. \quad (6)$$

By substituting (4) and (5) into (6) and applying to (1) limited to the second-order terms, we can have

$$g(x) = g(x-1) + \frac{1}{2}(B_x - B_{x-2}) + \frac{1}{8}(g(x+1) - 2g(x-1) + g(x-3)). \quad (7)$$

Applying (7) to actual Bayer pattern as shown in Fig. 2 gives

$$\hat{G}_x = G_{x-1} + \frac{1}{2}(B_x - B_{x-2}) + \frac{1}{8}(G_{x+1} - 2G_{x-1} + G_{x-3}) \quad (8)$$

where $\hat{G}_x$ is the estimated green value at x. This equation is the high-order interpolation for the left-side direction. Like this process, we can obtain the estimates for the other three directions, right, top, and bottom. The estimates of the missing pixels can be more accurate by using the second-order terms.

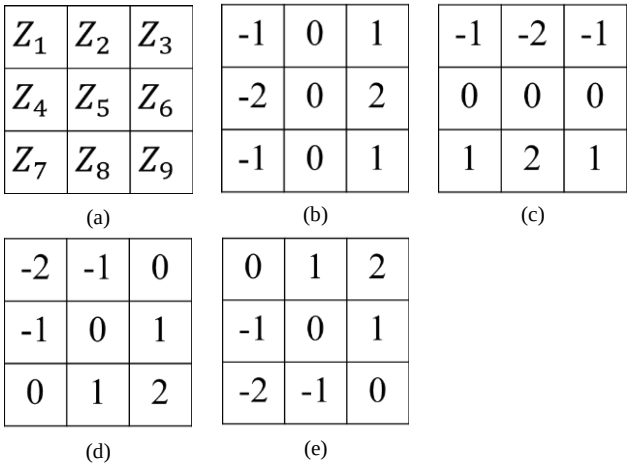

Fig 3. Sobel Masks with size of 3×3. (a) Pixel position for Sobel operator. (b) Sobel mask for horizontal direction. (c) Sobel mask for vertical direction. (d) Sobel mask for diagonal-right direction. (e) Sobel mask for diagonal-left direction.

III. PROPOSED ALGORITHM

A. Green Channel Interpolation

In previous section, we obtain 4 estimates using high-order interpolation. We decide the weights for 4 estimates to interpolate green channel in this section. The Sobel mask, a well-known and simple, is used to detect edges [9]. The reason we can adapt the Sobel mask is that CFA is symmetric. Fig. 3(a) shows the 3×3 mask. As shown in Fig. 3(b) and Fig. 3(c), the magnitudes of horizontal and vertical gradients are obtained by

$$H = \left|(Z_3 + 2Z_6 + Z_9) - (Z_1 + 2Z_4 + Z_7)\right|$$
$$V = \left|(Z_7 + 2Z_8 + Z_9) - (Z_1 + 2Z_2 + Z_3)\right| \quad (9)$$

where H is the magnitude for horizontal and V is the magnitude for vertical. The costs for horizontal and vertical are

$$C_h = M \otimes H(i-1:i+1, j-2:j+2)$$
$$C_v = M' \otimes V(i-2:i+2, j-1:j+1) \quad (10)$$

$$M = \begin{bmatrix} 0.5 & 1 & 2 & 1 & 0.5 \\ 1 & 2 & 4 & 2 & 1 \\ 0.5 & 1 & 2 & 1 & 0.5 \end{bmatrix} \quad (11)$$

where C_h is the horizontal cost, C_v is the vertical cost, M is the multiplication coefficient by distance and $\otimes$ denotes summation of element-wise matrix multiplication. Using above cost values, we can calculate the weights for 4 directions and interpolate green channel with these weights as follows:

$$w^T(i,j) = 1/C_v(i-1,j)$$
$$w^B(i,j) = 1/C_v(i+1,j)$$

ISBN: 978-988-19252-0-6
ISSN: 2078-0958 (Print); ISSN: 2078-0966 (Online)

$$w^L(i,j) = 1/C_h(i,j-1)$$
$$w^R(i,j) = 1/C_h(i,j+1) \quad (12)$$
$$\tilde{G} = \frac{w^T G^T + w^B G^B + w^L G^L + w^R G^R}{w^T + w^B + w^L + w^R}. \quad (13)$$

B. Green Channel Enhancement

After the green channel is interpolated, we enhance the green channel prior to the red and blue channel interpolation. To utilize the interchannel correlation between the green channel and other channels, color difference is employed and it is given as:

$$\tilde{C}_d(i,j) = \begin{cases} \tilde{G}(i,j) - R(i,j), & at\ R. \\ \tilde{G}(i,j) - B(i,j), & at\ B. \end{cases} \quad (14)$$

For more accurate information, we consider neighbor color differences as follows:

$$\bar{C}_d(i,j) = (w^T \tilde{C}_d(i-2,j) + w^B \tilde{C}_d(i+2,j) + w^L \tilde{C}_d(i,j-2) + w^R \tilde{C}_d(i,j+2))/w$$
$$w = w^T + w^B + w^L + w^R \quad (15)$$

where $\bar{C}_d$ is weighted sum of neighboring $\tilde{C}_d$. Using the results of (14) and (15), we can get the enhanced green channel as follows:

$$\hat{C}_d(i,j) = \alpha \tilde{C}_d(i-2,j) + (1-\alpha)\bar{C}_d(i,j) \quad (16)$$
$$\hat{G}(i,j) = \begin{cases} \hat{C}_d(i,j) + R(i,j), & at\ R. \\ \hat{C}_d(i,j) + B(i,j), & at\ B. \end{cases} \quad (17)$$

where α is experimentally determined as 1/3 and $\hat{G}$ is the enhanced green channel.

C. Red and Blue Channel Interpolation

Since the blue channel interpolation can be achieved in the same process, we only explain the red channel interpolation in this paper for simplicity. The red channel interpolation consists of two steps, because available pixels are different by the position. At first step, red pixels at blue pixel position are interpolated. However, valid red components are different from the green in CFA. We need the different Sobel operators to calculate gradients as shown in Fig. 3(d) and Fig. 3(e)

$$DR = \left|(Z_6 + 2Z_9 + Z_8) - (Z_2 + 2Z_1 + Z_4)\right|$$
$$DL = \left|(Z_2 + 2Z_3 + Z_6) - (Z_4 + 2Z_7 + Z_8)\right| \quad (18)$$

where *DR* is the magnitude for diagonal-right and *DL* is the magnitude for diagonal-left gradients. Each weight is calculated as follow:

$$w^{DR}(i,j) = 1/\sum_{y=-1}^{1}\sum_{x=-1}^{1} DR(i+x, j+y)$$
$$w^{DL}(i,j) = 1/\sum_{y=-1}^{1}\sum_{x=-1}^{1} DL(i+x, j+y). \quad (19)$$

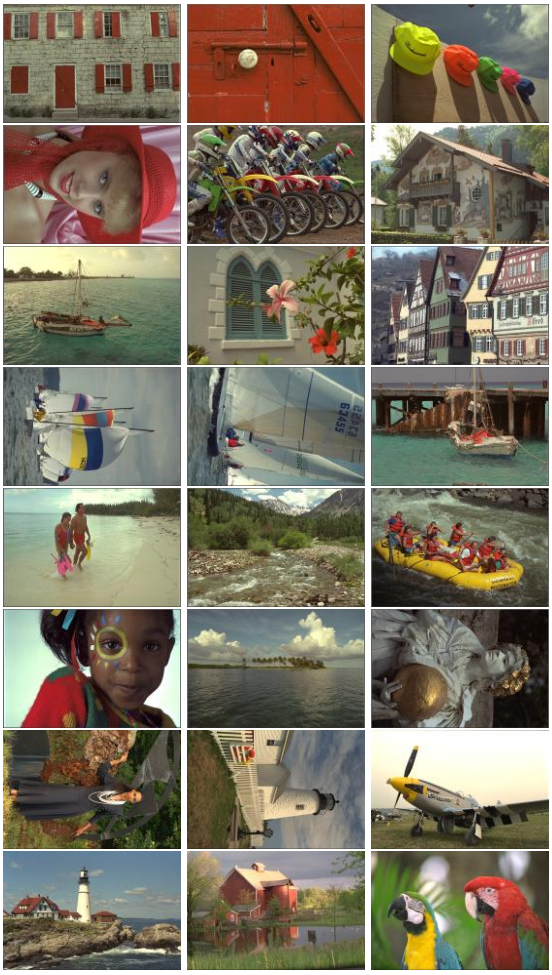

Fig 4. 24 Kodak images, referring to images 1 to 24 in a raster scanning order.

We assume that the enhanced green channel reliable, so we can get 4 estimates for the red channel using offset of the enhanced green channel

$$R^{TL}(i,j) = R(i-1,j-1) + (\hat{G}(i,j) - \hat{G}(i-1,j-1))$$
$$R^{TR}(i,j) = R(i-1,j+1) + (\hat{G}(i,j) - \hat{G}(i-1,j+1))$$
$$R^{BL}(i,j) = R(i+1,j-1) + (\hat{G}(i,j) - \hat{G}(i-1,j-1))$$
$$R^{BR}(i,j) = R(i+1,j+1) + (\hat{G}(i,j) - \hat{G}(i+1,j+1)). \quad (20)$$

And we can get red pixels at blue pixel position as follows:

$$\hat{R}(i,j) = (w^{DR}\hat{R}^{TL}(i,j) + w^{DL}\hat{R}^{TR}(i,j) + w^{DL}\hat{R}^{BL}(i,j-2) + w^{DR}\hat{R}^{BR}(i,j+2))/(2w^{DR} + 2w^{DL}). \quad (21)$$

Next step is the interpolation of red pixels at green pixel position. In this case, red pixels are classified into valid red pixels in CFA and interpolated pixels through the previous step. Also, this step uses offset of the enhanced green channel to get 4 estimates

$$R^T(i,j) = \hat{R}(i-1,j) + (\hat{G}(i,j) - \hat{G}(i-1,j))$$
$$R^B(i,j) = \hat{R}(i+1,j) + (\hat{G}(i,j) - \hat{G}(i+1,j))$$
$$R^L(i,j) = R(i,j-1) + (\hat{G}(i,j) - \hat{G}(i,j-1))$$
$$R^R(i,j) = R(i,j+1) + (\hat{G}(i,j) - \hat{G}(i,j+1)). \quad (22)$$

ISBN: 978-988-19252-0-6
ISSN: 2078-0958 (Print); ISSN: 2078-0966 (Online)

Finally, we can calculate the weighted summation of 4 estimates as follows:

$$\hat{R}(\mathrm{i},\mathrm{j}) = (w^T \hat{\mathrm{R}}^T(i,j) + w^B \hat{\mathrm{R}}^B(i,j) + w^L \hat{\mathrm{R}}^L(i,j) + w^R \hat{\mathrm{R}}^R(i,j))/w. \quad (23)$$

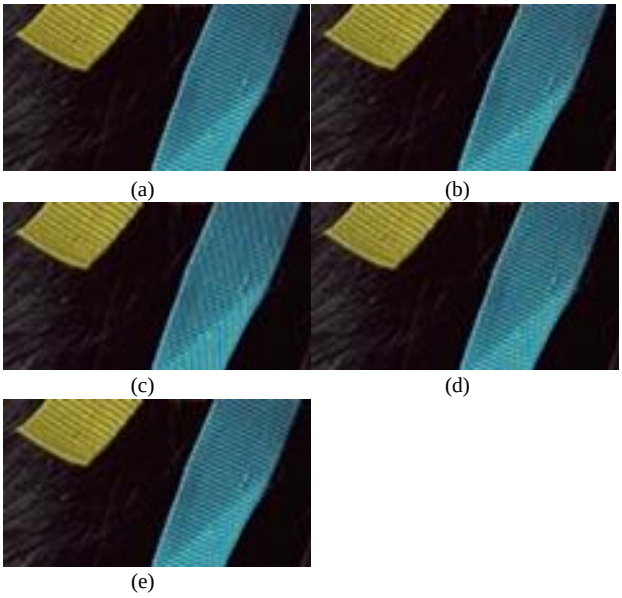

Fig 5. Comparison on outputs of Image 15. (a) origin. (b) VCD. (c) HOI. (d) IGD. (e) Proposed.

IV. Experimental Results

To evaluate the performance of our proposed algorithm, we compare ours with the three existing algorithms: VCD [5], HOI [6], IGD [7]. The 24 Kodak images shown in Fig. 4 were used for this experiment. These full color images were first down-sampled using Bayer pattern. Then, those were restored by the proposed algorithm and existing algorithms. We evaluate the performance of the proposed algorithm from two aspects, objective CPSNR and subjective visual quality comparison.

The CPSNR performances of the algorithms under comparison are listed in Table I. The best CPSNR value of each image is marked with bold. It is shown that the proposed algorithm and IGD achieved the best performance in terms of CPSNR. Also, it presents that the proposed algorithm is 0.12 dB higher CPSNR value on average than IGD.

Fig. 5 shows subjective visual quality of image 15. Fig. 5(a) is part of original image 15 and Fig. 5(b)-(e) are outputs of different demosaicing algorithms. The output images from HOI and IGD suffered from color artifacts. VCD and the proposed algorithm reduced relatively color artifacts. Compared to VCD, the proposed algorithm appears to produce visually more pleasant color image with more suppressed artifacts.

V. Conclusion

In this paper, we presented a new demosaicing algorithm based on high-order interpolation. By including the second-order terms, higher accuracy for four estimates can be achieved. In order to calculate gradients for each direction, the proposed algorithm used the Sobel operator. We added the green channel enhancement stage to improve the image quality. This work impacts on the red and blue channel's qualities. Our algorithm has 0.12 dB higher CPSNR than IGD algorithm. Also, comparison of subjective quality shows that the proposed algorithm produced demosaiced output images with minimal artifacts.

TABLE I.
Comparison of CPSNR Performance

Image	VCD	HOI	IGD	Prop.
1	35.39	36.74	**40.29**	39.86
2	39.34	40.87	40.65	**40.99**
3	41.46	42.43	42.67	**42.86**
4	39.96	40.91	40.79	**41.25**
5	35.72	37.67	37.95	**38.41**
6	37.65	38.95	**41.12**	40.31
7	40.93	42.82	42.44	**42.94**
8	33.49	34.96	**37.36**	37.05
9	41.24	42.46	43.27	**43.44**
10	40.63	42.35	42.72	**43.12**
11	37.72	39.30	40.72	**40.92**
12	42.02	43.18	**44.16**	44.01
13	31.78	32.88	**36.20**	35.94
14	35.93	37.07	36.64	**36.99**
15	38.72	39.05	39.54	**40.03**
16	41.56	42.68	**44.81**	43.74
17	39.54	40.79	41.79	**42.24**
18	34.94	36.28	37.36	**37.89**
19	38.58	39.88	**41.70**	41.46
20	39.03	40.53	41.46	**41.85**
21	36.61	38.06	40.27	**40.37**
22	36.60	37.88	38.19	**38.69**
23	42.16	43.40	42.69	**43.04**
24	33.34	33.92	34.98	**35.21**
Avg.	38.10	39.38	40.41	**40.53**

References

[1] B. E. Bayer, "Color imaging array," *U.S. Patent 3971065*, Jul.1976.
[2] D. R. Cok, "Signal Processing method and apparatus for producing interpolated chro- minance values in a sampled color image signal," U.S. Patent 4642678, Feb. 1987.
[3] S.C. Pei and I. K. Tam, "Effective color interpolation in CCD color filter arrays using signal correlation," *IEEE Trans. Circuit Syst. Video Technol.*, Vol.13, No.6, pp.503-513, Jun. 2003.
[4] J. F. Hamilton and J. E. Adams, "Adaptive color plane interpolation in single sensor color electronic camera,"U.S. Patent 5 629 734,1997
[5] K. H. Chung and Y. H. Chan, "Color demosaicing using variance of color differences," *IEEE Trans. Image Process.*, vol. 15, no. 10, pp. 2944-2955, Oct. 2006.
[6] J. S. J. Li, and S. Randhawa, "Color filter array demosaicking using high order interpolation techniques with a weighted median filter for sharp color edge preservation," *IEEE Transactions on Image Processing*, Vol.18, No.9 ,2009.
[7] K. H. Chung and Y. H. Chan, "Low-complexity color demosaicing algorithm based on integrated gradients," *J. Electron. Imag.*, vol. 19, no. 2, p. 021104-1-15, Jun. 2010.
[8] E. Kreyszig, *Advanced Engineering Mathematics*. New York: Wiley, 1999.
[9] R. Gonzalez, R. Woods, *Digital Image Processing*, Prentice Hall, 2009.

ISBN: 978-988-19252-0-6
ISSN: 2078-0958 (Print); ISSN: 2078-0966 (Online)